ARTICLE IN PRESS

Enhancing serpentine dissolution kinetics for mineral carbon dioxide sequestration

Samuel C.M. Krevor*, Klaus S. Lackner

Department of Earth and Environmental Engineering, Columbia University, 918 Mudd Building, New York City, NY 10027, USA

ARTICLE INFO

ABSTRACT

Mineral carbon dioxide sequestration binds carbon dioxide by reacting it with magnesium silicate minerals to form solid magnesium carbonates that are ready for disposal. Research on mineral sequestration has focused on enhancing process kinetics in aqueous processing schemes. High costs of these processes are associated with mineral processing, such as ultrafine grinding, or the consumption of acids and bases, which are required to speed up silicate mineral dissolution kinetics. Neutral organic salts such as sodium oxalate, and citrate enhance dissolution kinetics of serpentine in the circum-neutral pH range appropriate for mineral carbonate precipitation and have potential for use in an enhanced carbonation process. Concentration and temperature dependencies for the dissolution of antigorite serpentine in the presence of the citrate ion are experimentally derived under weakly acidic conditions. Rates are shown to be several orders of magnitude higher in the presence of citrate than in the weakly acidic solution alone.

© 2011 Elsevier Ltd. All rights reserved.

1. Introduction

Mineral carbon dioxide sequestration is a proposed greenhouse gas mitigation technology that binds carbon dioxide (CO_2) by reacting it with calcium or magnesium silicate minerals to form solid magnesium or calcium carbonates that are ready for disposal (Lackner et al., 1995; Seifritz, 1990). Mineral sequestration offers virtually unlimited capacity to permanently store CO_2 in an environmentally benign form (Goff and Lackner, 1998; Krevor et al., 2009). It takes little effort to verify and monitor the successful storage of CO_2. These characteristics are unique among greenhouse gas disposal technologies.

For reasons of mineral availability, cation concentration, and reactivity, the focus of mineral carbonation research has been on the carbonation of rocks rich in the magnesium silicate minerals serpentine (Eq. (1)) and olivine (Eq. (2)).

$$Mg_3Si_2O_5(OH)_4 + 3CO_2 \rightarrow 3MgCO_3 + 2SiO_2 + 2H_2O \qquad (1)$$

$$Mg_2SiO_4 + 2CO_2 \rightarrow 2MgCO_3 + SiO_2 \qquad (2)$$

Although thermodynamic equilibrium at conditions near the surface of the earth favor carbonate minerals, reaction kinetics are very slow. Thus, special conditions are required to perform the reactions on time scales relevant to industrial CO_2 emission. Various process schemes have been developed to enhance reaction kinetics, including heat-pretreatment and pulverization of the minerals, but energy consumption of these processes is high (Gerdemann et al., 2007; Newall et al., 1999; Huijgen et al., 2007).

Research in mineral sequestration has focused mainly on aqueous carbonation processes (Fig. 1). In the most promising aqueous processes, energy consumption associated with the grinding of reactant minerals to very fine grain sizes (4 μm) make up 75% of the total energy costs (Gerdemann et al., 2007; Newall et al., 1999; Huijgen et al., 2007). As a result, fine grinding is also the main contributor to high cost estimates, a factor of 3–10 times higher than costs associated with underground injection (IPCC, 2005). Increasing the reaction kinetics will allow for the use of coarser-grained materials (or the achievement of higher carbonation yields at a given grain size), thereby decreasing the energy costs per net amount of CO_2 sequestered.

Aqueous carbonation of mineral silicates involves two steps: Dissolution of cations from the silicate minerals into solution followed by nucleation and growth of carbonate precipitate (Huijgen et al., 2006; Chizmeshya et al., 2003; Teir et al., 2007; Guthrie et al., 2001; Jarvis et al., 2009). Eqs. (3) and (4) show representative dissolution and carbonate precipitation reactions in an acidic system.

$$\frac{1}{3}Mg_3Si_2O_5(OH)_4 + 2H^+ \rightarrow Mg^{2+} + \frac{2}{3}SiO_2(aq) + \frac{2}{3}H_2O \qquad (3)$$

$$Mg^{2+} + HCO_3^- \rightarrow MgCO_3(S) + H^+ \qquad (4)$$
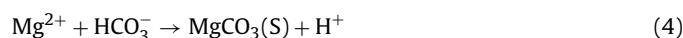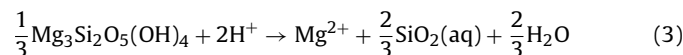
The exact phase of the initial precipitate may not be magnesite, but hydromagnesite, nesquehonite, or any number of magnesium carbonate phases depending on process conditions (Hänchen et al., 2008). Both the dissolution of silicate minerals and the formation of

* Corresponding author. Present address: 367 Panama Street, 065 Green Earth Sciences, Stanford, CA 94305, USA. Tel.: +1 212 3658058; fax: +1 650 725 2099.
E-mail address: skrevor@stanford.edu (S.C.M. Krevor).
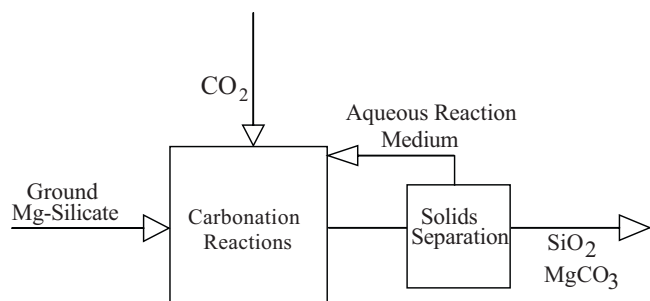
Fig. 1. Schematic of an aqueous direct carbonation process for mineral carbon sequestration.

carbonate minerals are pH dependent, as can be seen with the presence of the hydrogen ion as a key reaction component in Eqs. (3) and (4). Basic silicates such as serpentine and olivine are increasingly soluble with increasing acidity in solution. Carbonate mineral formation, however, is only possible if the solution is supersaturated with respect to cations and carbonate (or bicarbonate) ions. Acidity decreases the activity of carbonate ions in solution since protonation of the carbonate ion leads to the formation of bicarbonate ions. At very low pH bicarbonate ions are converted to carbonic acid which then decomposes into CO_2 and water.

If dissolution and precipitation are to take place simultaneously in an aqueous system, conditions must exist such that the system is undersaturated with respect to the silicate mineral but supersaturated with respect to the carbonate phase (Fig. 2). Under
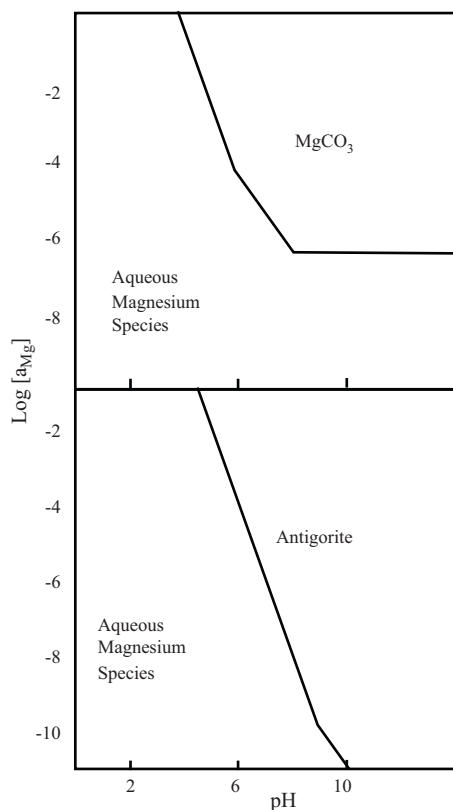
Fig. 2. Solubility diagrams for antigorite serpentine and magnesium carbonate. Diagrams show antigorite serpentine or magnesite stability fields as a function of solution pH (horizontal axis) and magnesium ion activity (vertical axis). Equilibria are calculated using Geochemist Workbench software. Both are at 120 °C and a CO_2 fugacity of 20 atmospheres. In the serpentine graph, solution is always supersaturated with respect to amorphous silica, and the talc phase is suppressed. The magnesite graph contains no silica and no phases are suppressed.

these conditions, which run from weakly acidic to weakly basic, dissolution kinetics for magnesium silicate minerals are overwhelmingly rate-limiting (Hänchen et al., 2008; Bales and Morgan, 1985; Oelkers and Schott, 2009; White and Brantley, 1995). Slow silicate dissolution kinetics are precisely why high yields of carbonate production in short time periods have only been achieved with the relatively reactive olivine, and only after the dissolution is enhanced through the energy-intensive attrition grinding stage (Gerdemann et al., 2007).

Some have sought to overcome slow dissolution kinetics by dissolving the silicate minerals in strongly acidic solutions. This results in the requirement to add base to the leachate solution in subsequent process stages so as to allow for the formation of the solid carbonate product. These processes have been described as pH-swing processes (Teir et al., 2007; Kim et al., 2009; Maroto-Valer et al., 2005; Park and Fan, 2004), but it is necessary to add a 1:1 or 2:1 stoichiometric ratio of base to CO_2 to complete the process and the amounts of replacement chemical (acid and base) are so large that a single 500 MW coal-fired power plant would require a significant percentage of the current world production of acids and bases (Newall et al., 1999). Onsite recovery of the acid and base is possible, but requires substantial energy inputs. This energy input may not be prohibitively expensive considering that the addition of hydrochloric acid resulted in a similarly exothermic reaction (House et al., 2007), but it may be possible to avoid this energy transfer completely if one can find a way of dissolving the serpentine rock at an essentially neutral pH, i.e. in a solution more weakly acidic than carbonic acid.

Eq. (5) is an expression for the surface area specific dissolution rate, r [mol cm^{-2} s^{-1}], as a function of solution species activity, a_i [–], and temperature T [K] (Eq. (5)) and is appropriate for system conditions in which the dissolution reaction is far from equilibrium.

$$r = Aa_i^{n_i} \exp\left(\frac{-E_a}{RT}\right) \tag{5}$$

where A [mol cm^{-2} s^{-1}] is a rate constant, in solution, n_i [–] is reaction order with respect to the solution species, i, E_a [kJ mol^{-1}] is the activation energy of the dissolution reaction. R is the universal gas constant. The solution species dependence, n, can be derived by obtaining dissolution rates in solutions with various species activities. Published values for the proton promoted dissolution of serpentine and olivine are provided in Table 1.

Compared to dissolution rates in strongly acidic systems, proton-promoted dissolution kinetics will be slow under the weakly acidic to basic conditions that allow for carbonate precipitation, because values for the pre-exponential factor, A, are small and a_{H^+} will be on the order of 10^{-5} or less. Fast dissolution kinetics could be achieved under these conditions, however, if dissolution is promoted by some solution species, i, other than the proton.

Both organic and inorganic ionic (non-acidic) species can promote the dissolution of silicate minerals (Teir et al., 2007; Bales and Morgan, 1985; Park and Fan, 2004; Hänchen et al., 2006; Pokrovsky et al., 2009; Olsen and Rimstidt, 2008; Liu et al., 2006; Grandstaff, 1986; Carey and Ziock, 2004; Kakizawa et al., 2001; Wogelius and Walther, 1991; Allen and Smith, 1994; Bonifacio et al., 2001; Kline and Fogler, 1981). These studies have shown that the dissolution rate of olivine is enhanced in the presence of EDTA, ascorbate, potassium hydrogen pthalate, oxalate, citrate, tannate, and acetate (Hänchen et al., 2006; Olsen and Rimstidt, 2008; Grandstaff, 1986; Wogelius and Walther, 1991). It has also been found that the presence of organic ions EDTA, oxalate, and citrate can enhance initial rates of dissolution of serpentine (Bales and Morgan, 1985; Park and Fan, 2004).

In this study, we have sought to identify non-acidic ionic solution species (e.g. the citrate ion) that enhance the silicate dissolution without inherently being consumed in chemical reactions,

Table 1
Dissolution rates of olivine and serpentine (Teir et al., 2007; Bales and Morgan, 1985; Hänchen et al., 2006).

Mineral	Pre-exponential, A [mol cm^{-2} s^{-1}]	Reaction order, n	Activation energy, E_a [kJ mol^{-1}]
Olivine	0.0854	0.46	52.9
Serpentine	0.028	0.24	70

and that work in the weakly acidic to weakly basic pH conditions that are suitable for the precipitation of carbonate phases. In addition, we have focused our experimental work on enhancing the dissolution of serpentine, among the least reactive and most abundant of the ultramafic minerals (Krevor et al., 2009; Bales and Morgan, 1985).

2. Materials and methods

Experimental work has focused on enhancing the dissolution of the antigorite serpentine (referred to as serpentine from here forward) in weakly acidic solutions. Serpentine has been dissolved in various solutions of neutral salts in the presence of a constant CO_2 pressure over the solution with the goal of identifying those salts that accelerate the dissolution process.

2.1. Materials and experimental procedure

Starting material was untreated serpentine collected from tailings at the Belvidere mountain asbestos mine in Northern Vermont. Two size distributions were sieved from tailings (Fig. 3). One had a volume-normalized mean diameter of 217 μm. This distribution will be referred to as distribution 217. Another distribution had a volume-normalized mean diameter of 189 μm. This distribution will be referred to as distribution 189. The distributions were measured using a Beckman Coulter LS 13-320 laser diffraction particle size analyzer. Surface area was determined using the nitrogen BET adsorption method, and was found to be 2.94 m^2/g for the finer distribution and 2.70 m^2/g for the coarser distribution. Analysis for major oxide content was performed by SGS Mineral Services using X-ray fluorescence. Iron content (as Fe_2O_3) was 7.78%, as a magnetic iron-oxide phase separate from the serpentine. MgO content was 39.1% and SiO_2 was 37.9% by weight. The balance consisted of Al_2O_3 (1.02%), CaO (0.53%), Na_2O (0.05%), K_2O (0.01%), MnO (0.11%), TiO_2 (0.02%), Cr_2O_3 (0.39%), and mass loss on ignition of 12.1%. Qualitative XRD analysis, also performed by SGS Mineral Services, identified serpentine as the only magnesium-bearing phase.
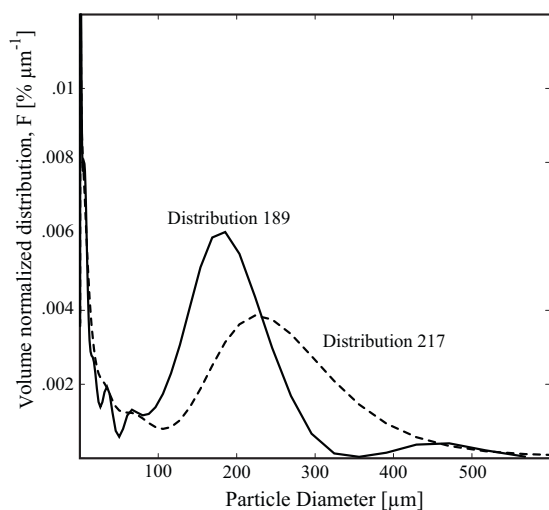
One set of experiments was used to compare the dissolution in different salt solutions. For these experiments 3 g of serpentine was reacted in solutions of 1 M NaCl (Fisher C.A.S. 7647-14-5), 1 M NH_4Cl (Fisher C.A.S. 12125-02-9), 0.1 M trisodium citrate (Fisher C.A.S. 6132-04-3), 0.1 M disodium EDTA (Fisher C.A.S. 6381-92-6), 0.1 M sodium oxalate (Fisher C.A.S. 62-76-0), and 0.5 M sodium acetate (Fisher C.A.S. 6131-90-4) under an atmosphere of 20 bars of CO_2 pressure at 90 °C. Two experiments, one with 1 M NH_4Cl and one with no salts in solution, were performed under 20 bars of pressure in an N_2 atmosphere at 90 °C (Table 2).

Another set of experiments was performed to understand the salt concentration and temperature dependence of citrate promoted dissolution. To obtain the temperature dependence of the citrate-promoted dissolution, 1 g of serpentine was dissolved in 0.5 M trisodium citrate solutions at 60 °C, 70 °C, 90 °C, and 120 °C under 20 bars of pressure from a CO_2 gas cylinder. To obtain the citrate ion activity dependence, 1 g of serpentine was dissolved in 0.05 M, 0.1 M, 0.3 M, and 0.5 M trisodium citrate solutions at 90 °C under 20 bars of pressure from a CO_2 gas cylinder. The experimental conditions of this set of experiments are provided in Table 3.

In all experiments, ground serpentine is reacted in 1 kg of deionized H_2O with dissolved salts in a Parr 4520 stainless steel batch autoclave with temperature, pressure, and stirring control. Experiments have been performed under 20 bars of pressure, with a CO_2 or N_2 atmosphere as specified. Salts are dissolved fully in solution, after which time the serpentine sample is added and the clock started. The reactor is closed, placed in the heater and subsequently purged and pressurized with CO_2 from a gas cylinder. The heater is turned on and experiments take between 20 and 45 min to reach steady state temperature. As the reactor heats up, pressure exceeding 20 bars is relieved by briefly opening a valve on the reactor. Stirring is started simultaneously with the heater and was run at 600 rpm. Experiments last from 6 to 24 h and samples are drawn periodically during the experiment through a dip tube with a stainless steel 0.2 μm filter on the submerged end. Each sample results in a solution loss of about 5 g and no more than 10% of the solution is drawn throughout any given experiment.

Samples are analyzed for magnesium content using a Buck Instruments AA flame spectrophotometer with an error of 5% of the measured concentration. The instrument can characterize magnesium concentrations accurately in a range of 0.1–1 ppm and samples were diluted by a factor of 100 for analysis. Dissolved silica for some of the experiments was measured using the molybdenum yellow method using a Perkin Elmer Lambda 25 spectrometer. The silica measurement was calibrated for the measurement of Si con-

Fig. 3. Volume normalized particle size distributions (% of total volume of sample represented by particles of a given diameter) of samples used in this study.

Table 2
Conditions for experiments in which dissolution in different salt solutions was tested. All experiments performed at 90 °C, under 20 bars of pressure, with 3 g of serpentine from PSD 189 in 1 kg of deionized water.

Experiment	Atmosphere	Salt	Salt conc. [mol l^{-1}]
a	CO_2	Oxalate	0.1
b	CO_2	EDTA	0.1
c	CO_2	Citrate	0.1
d	CO_2	NH_4Cl	0.1
e	N_2	NH_4Cl	0.1
f	CO_2	NaCl	0.1
g	CO_2	None	N/A
h	N_2	None	N/A
i	CO_2	Acetate	0.5

Table 3
Experimental conditions and best-fit model parameters for the dissolution of serpentine in citrate solutions at various temperatures and citrate concentrations. All experiments were performed with 1 g of serpentine in 1 kg of deionized water.

Experiment number	Temperature [°C]	Citrate concentration [mol l⁻¹]	Best-fit rate [cm s⁻¹]	PSD [mean diameter]
1	90	0.5	1.64×10^{-07}	189 μm
2	120	0.5	3.43×10^{-07}	189 μm
3	70	0.5	5.06×10^{-08}	189 μm
4	60	0.5	3.97×10^{-08}	217 μm
5	90	0.5	1.68×10^{-07}	217 μm
6	90	0.1	6.44×10^{-08}	189 μm
7	90	0.05	4.15×10^{-08}	189 μm
8	90	0.3	2.08×10^{-07}	217 μm

centrations between 0.4 and 2 ppm by weight and samples were diluted by a factor of 100 for analysis. Through repeated measurements it was found that Si concentrations were reproducibly measurable to within 10 ppm in the final concentrations, or 11–15% precision. Dissolution rates are calculated when appropriate by fitting a shrinking particle model to the magnesium data as described below.

The pH could not be measured in situ. In addition, the thermodynamic properties of the citrate molecule have not been measured in the temperature and solution composition range required to model precise pH values for the experimental conditions used. A maximum pH range in the absence of the organic compounds was constructed based on the CO_2 pressure and stoichiometric dissolution of our serpentine sample using the Geochemist's Workbench software package using the B-dot equation to calculate activity coefficients (Bethke and Yeakel, 2007). Calculations were performed in the absence of salts and with 1 M NaCl solutions to see the impact of ionic strength on the pH. The maximum range in pH that can be obtained through these calculations is from 3.55 when no dissolution has taken place to 5.2 when 100% of 1 g of serpentine with chemical composition as given by the analyzed sample has been dissolved. Solutions are acidic because of the CO_2 atmosphere. As serpentine dissolves, release of magnesium with the associated hydroxyl groups into solution raises the pH, and is partially offset by an increased dissolution of CO_2.

The organic salts in solution could provide buffering capacity that prevents the pH from falling below the pK_a of the acidic components of the salt. In the case of the trisodium citrate at 25 °C this would provide buffering capacity at pH values of 6.4, 4.76, and 3.13. This would weaken proton-promoted dissolution and thus rely even more on the catalytic effect of the organic anions. Even at pH value of 3.55, which is the lowest it could reasonably be expected to be, the proton-promoted dissolution rates would be too slow for observation by this study (Stoll and Blanchard, 1990).

2.2. Modeling the dissolution rate

The authors took the commonly used approach of using experimental conditions such that the system was far from equilibrium with respect to serpentine solubility (Hänchen et al., 2008; Oelkers and Schott, 2009; White and Brantley, 1995; Palandri and Kharaka, 2004). Under these conditions, Eq. (5) is an appropriate expression for the dissolution rate. In the experiments where the dissolution rate was modeled as a function of citrate concentration, the rate, r, is defined as moles of serpentine cm⁻² s⁻¹ released into solution. The release of the magnesium ion is taken as a proxy for total mineral dissolution, and the release of approximately 3 mol of Mg is representative of the dissolution of 1 mol of serpentine. The solution species, a_i, is taken to be citrate ion concentration.

The activation energy, E_a, of the dissolution may be derived by obtaining dissolution rates at various temperatures (Hänchen et al., 2008; Oelkers and Schott, 2009; White and Brantley, 1995; Palandri and Kharaka, 2004). Plotting the natural log of the rate against the inverse of the temperature, the activation energy is determined from the slope of the line (Eq. (6)).

$$\ln r = \ln A a_i^n - \frac{E_a}{RT} \tag{6}$$

For deriving the surface-normalized dissolution rate of a mineral in experiments in which large percentages (>10%) of the sample are dissolved and the specific surface area of the sample changes appreciably throughout the experiment, the population balance framework is useful (Hänchen et al., 2007). Using this technique, the particle size is often described by a single characteristic length, L, such as the diameter or radius of the particle. The distribution of particles, $F(L,t)$, represents the number of particles in the sample as a function of the characteristic particle length, L, and time, t (Leblanc and Fogler, 1987). The dissolution rate, D, is defined as the rate of change of the characteristic length of a given particle:

$$\frac{dL}{dt} = -D(L) \tag{7}$$

This dissolution rate is related to the surface-normalized dissolution rate (Eq. (5)) through the relationship between the surface area and the characteristic length (Eq. (8)).

$$\frac{dL}{dt} = -D = \frac{-rk_a}{3\rho k_v} \tag{8}$$

where r [mol m⁻² s⁻¹] is the chemically controlled reaction rate (Eq. (5)), and ρ [mol m⁻³] is the molar density of the particle. k_a [–] and k_v [–] are shape factors relating the surface area and volume to the characteristic length respectively. Assuming spherical particles with L as the diameter, $k_a = \pi$ and $k_v = \pi/6$. If the shape factors are the same for all particles, then the linear dissolution rate, D, is independent of characteristic length. This is implicit in the assumption of a surface-reaction controlled dissolution process (Hänchen et al., 2007).

Assuming no breakage or agglomeration of particles occurs, the time-varying change of the distribution F of particles with a characteristic length between L and $L + dL$ is given by the balance of the number of particles entering this size regime and the number of particles leaving this size regime via dissolution given by $D(L + dL)$ and $D(L)$ respectively:

$$\frac{\partial}{\partial t}[F(L, t)] = D \frac{\partial}{\partial L}[F(L, t)] \tag{9}$$

Because D is independent of the characteristic length it can be taken out of the differential. This equation has the form of first-order wave equation and may be solved using the method of characteristics (Leblanc and Fogler, 1987).

Once the initial particle size distribution, F, of a sample is measured, and a geometry is either assumed or measured so that shape factors may be defined, the dissolution of that sample at any rate, D (or r), may be modeled. Obtaining the dissolution rate of a sample from an experiment is a matter of finding the value of the dissolution rate D that closest fits the experimental data.
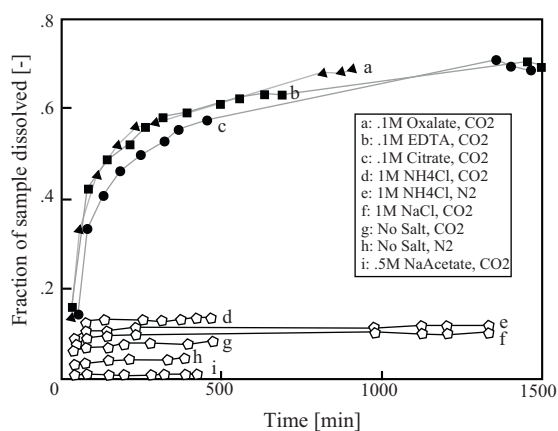
Fig. 4. Dissolution of serpentine in various salt solutions. All experiments were performed at 90 °C and under 20 bars of CO_2 except for the experiment labeled 'No Salt, N_2' and '1 M NH_4Cl, 20 atm N_2', which were performed under 20 bars of N_2.

All samples were taken after the experiment reached steady state temperature, which took between 20 and 45 min depending on the temperature. Because of the non-steady state startup period, two parameters must be varied in the model to obtain fits: the dissolution rate and the effective start-time of the model (the time relative to the experimental time at which there would have been zero dissolution if the dissolution rate would have been constant in the startup period). Two parameter least-squares regression is performed minimizing the error between the model and the data to obtain best fits. Uncertainty on individual rate values are taken to be the locus of rate fits that result in an average residual of less than 2 standard deviations of the residuals in the best-fit rate. Only samples taken after 20% of the solid material has dissolved into solution were used in the regression, ensuring that the fines or other irregularities associated with the startup of the experiment were not impacting the derivation of the dissolution rate.

3. Results

Results are provided as the fraction of the sample dissolved versus time from when the reactor was closed. The fraction of the mineral dissolved is calculated as the ratio of magnesium in solution to total magnesium in the sample. In three experiments where it was measured, silica dissolution was found to be congruent with magnesium, until the solution was saturated with respect to silica, justifying the use of magnesium as a proxy for total mineral dissolution (Fig. 5).

3.1. Dissolution in different salt solutions

In experiments with NaCl, NH_4Cl, or acetate, there is no discernible enhancement in dissolution rate over experiments with no salts in solution (i.e. a CO_2–water system) (Fig. 4). The steady-state dissolution rates are too slow for quantification within the time frame of the experiments. In experiments with citrate, EDTA, and acetate, dissolution proceeds rapidly. At least in the case of citrate at higher temperatures, 100% dissolution can be achieved within 24 h (Fig. 5).

3.2. Temperature dependence of citrate promoted dissolution

One gram samples of serpentine were dissolved in 0.5 M trisodium citrate solutions with 20 bars of pressure from a CO_2 gas cylinder at 60 °C, 70 °C, 90 °C, and 120 °C. Experiments were performed with both grain size distributions to check for consistency.
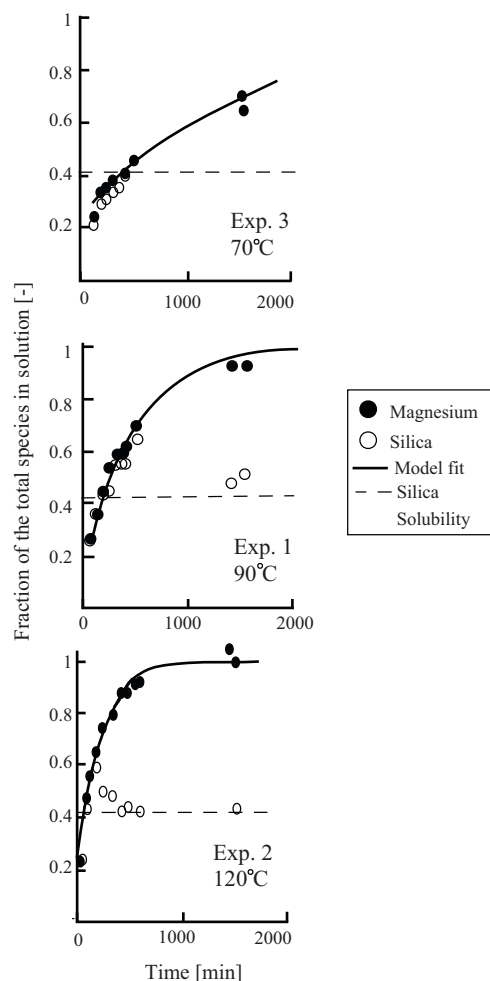
Fig. 5. Dissolution of serpentine in 0.5 M Na_3 Citrate at 70°, 90°, and 120 °C under 20 bars of pressure from a CO_2 gas cylinder. PSD 189. Solid line shows best rate fit. Filled circles show experimental data for magnesium concentration. Open circles show experimental data for aqueous silica concentration. Concentrations are normalized to the fraction of total possible concentration in solution as described in the text. The dotted line shows the solubility of amorphous silica at 25 °C.

Rates were fit to experimental data using the shrinking particle model and population balance framework. Graphs showing the model fit to data for experiments with PSD 189 and at 70 °C, 90 °C, and 120 °C are shown in Fig. 5. Best-fit parameters for all experiments are given in Table 3. Dissolution increased with increasing temperature. The activation energy was derived using Eq. (6), fitting a line to a plot of the natural log of the rate versus the inverse of temperature (Fig. 6). The activation energy of the dissolution was found to be 42 ± 15 kJ mol^{-1}. This represents a 27 kJ mol^{-1} lower activation energy than what has been observed for the proton-promoted dissolution of serpentine (Table 1).

3.3. Citrate concentration dependence of dissolution

One gram samples of serpentine were dissolved in 0.05, 0.1, 0.3, and 0.5 M trisodium citrate solutions, at 90 °C and 20 bars of pressure from a CO_2 gas cylinder and best-fit model parameters are given in Table 3. Dissolution increased with increasing citrate concentration. The concentration dependence was found to vary with the log of the rate proportional to the log of citrate concentration with an order of dependence of 0.65 ± 0.1 (Fig. 6).
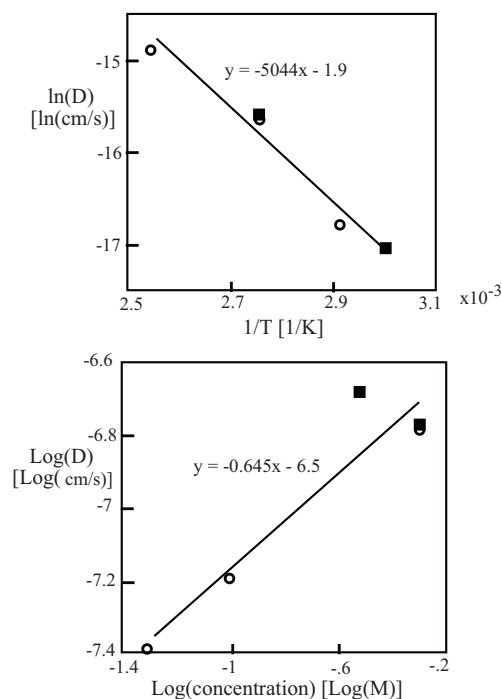
Fig. 6. Above: The natural log of best-fit rates of dissolution experiments in 0.5 M citrate solutions at different temperatures plotted against the inverse of temperature [Kelvin]. Below: Log (base 10) of best-fit rates of dissolution experiments at 90 °C and different citrate concentrations plotted against the log of the citrate concentration in solution. Circles show results obtained with PSD 189 and squares show results obtained with PSD 217. Regressions were performed using all of the experiments. Data points for the graph are given in Table 3.

3.4. Silica dissolution

Aqueous silica was measured for experiments with citrate in which the temperature was varied between experiments. Results are shown in Fig. 5. Dissolution is stoichiometric with magnesium dissolution until a silica concentration reaches 90–94 ppm Si by weight in solution (equivalent to a fraction dissolved of 0.58–0.6). After this, aqueous silica concentration drops and maintains concentrations between 65 and 80 ppm. This observation is consistent with the precipitation of a silica phase from solution after reaching a threshold supersaturation. The final Si concentration is close to what would be expected given the solubility limit of amorphous silica at 25 °C (115 ppm SiO_2 or about 65 ppm Si; Morey et al., 1964; Gunnarsson and Arnorsson, 2000); the temperature at which the samples were analyzed. The solubility of amorphous silica increases with temperature and could not have been exceeded with the 1 g samples at the elevated temperatures of the experiments (Gunnarsson and Arnorsson, 2000). Thus, it is likely that a precipitation event occurred during or after the fluid sample was taken from the reactor.

3.5. Comparison with other dissolution rates

Mineral dissolution rate laws are generally published as a rate normalized to a surface area in units of [mol cm^{-2} s^{-1}] where the surface area is measured using the nitrogen or argon BET absorption technique. A transformation of rates observed in this study to a rate normalized to BET surface area is required to make a comparison. This is done by correlating the measured BET surface area to the calculated geometrical surface of particles area using the measured radii distribution and assuming a specific grain geometry. A unitless roughness factor, γ, is included in the area shape factor to account
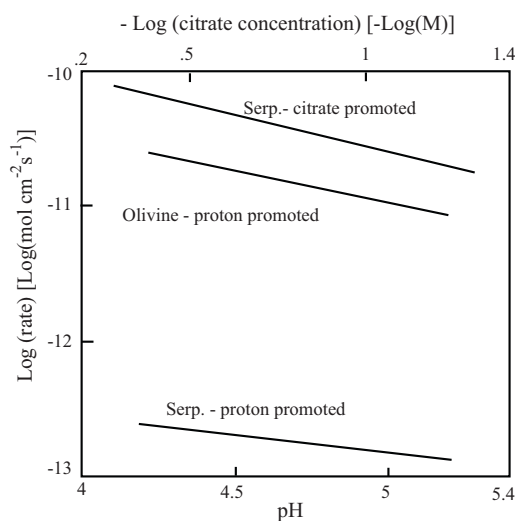
Fig. 7. Dual horizontal axis graph showing the modeled dissolution rates of serpentine in citrate (top horizontal axis applies), serpentine in acid solutions, and olivine in acid solutions (bottom horizontal axis applies) as a function of the concentration of dissolution promoting species at 90 °C at approximate solution conditions obtained in the experiments. Rate law of the form of Eq. (5) with parameters from Table 1 and as derived from citrate dissolution experiments. In this comparison, citrate-promoted dissolution rate of serpentine is several orders of magnitude higher than the proton-promoted dissolution as observed by others.

for this difference (Eq. (10)) (White and Brantley, 1995).

$$k_a = \pi\gamma \tag{10}$$

The roughness factor may be obtained by dividing the observed (BET) surface area, A_{BET}, by the surface area that would be calculated from the characteristic length distribution assuming spherical particles (Eq. (11)). Combining the observed size distribution and surface area measurement of our samples, γ was found to be 29.2.

$$\gamma = \frac{A_{BET}}{\sum_{i=1}^{N} \pi L_i^2} \tag{11}$$

The roughness factor is sensitive to the characterization of the fine particles in the distribution. A large percentage of the geometrically calculated surface area is associated with particles below 100 μm and is sensitive to arbitrary sensitivity thresholds of the laser diffractometer in observing small particles. The best-fit radial dissolution rates, D, and thus the temperature and chemical concentration dependencies, are not sensitive to this as the model fits to experimental data are dependent on the characterization of the volume-distribution, dominated by larger particles well within range of the detection thresholds of the instrument. The transformation of the radial dissolution rate to the BET normalized dissolution rate, however, is quite sensitive to the characterization of the very fine-grained material. For this and other reasons, inter-laboratory rate comparisons are generally only repeatable within one order of magnitude (e.g. Oelkers and Schott, 2009; White and Brantley, 1995).

With that qualification in mind, the concentration and temperature dependence of citrate promoted dissolution derived in this study can be used to construct a rate law of the form of Eq. (5). With the derived parameters, activation energy $E_a = 42$ kJ mol^{-1}, concentration dependence $n = 0.65$, and pre-exponential $A = 1.32 \times 10^{-4}$ mol cm^{-2} s^{-1}. Fig. 7 shows a comparison of the 90 °C surface-area normalized dissolution rates, r [mol cm^{-2} s^{-1}], of olivine as a function of pH (Hänchen et al., 2006), serpentine as a function of pH (Teir et al., 2007; Bales and Morgan, 1985), and serpentine as a function of citrate concentration (this study). Serpentine dissolution at high concentrations of citrate and

under pH conditions used in this study appears to be 2–3 orders of magnitude faster than what is predicted by other studies for proton-promoted dissolution alone. While error in this comparison introduced by the issues with the characterization of the surface discussed above may be as much as an order of magnitude, it is clear that the citrate-promoted dissolution achieves higher rates of dissolution under the conditions used in this study than what would have been observed with proton-promoted dissolution alone.

4. Discussion and conclusions

Dissolution experiments in inorganic and acetate salt solutions show that dissolution of serpentine in these solutions is of little interest for an industrial scale mineral carbon sequestration process. Enhanced dissolution in organic acids and in citrate solutions in particular has been previously observed for silicate minerals (Hausrath et al., 2009; Bales and Morgan, 1985; Hänchen et al., 2006; Pokrovsky et al., 2009; Olsen and Rimstidt, 2008; Liu et al., 2006; Grandstaff, 1986; Carey and Ziock, 2004; Wogelius and Walther, 1991). Liu et al. (2006) have suggested in the case of the mineralogically simpler olivine group, that the enhancement is due to the anion's replacement of water as a ligand destabilizing the Mg–O bond at the oxygen site that bridges silica and magnesium components of the mineral, the suggested rate-limiting step in the dissolution process. Others have suggested that there is a direct interaction between the organics and the silica components of the mineral even without the formation of Si–ligand complexes in the bulk solution (Mavredaki et al., 2007; Bennett et al., 1988; Bennett, 1991; Fein and Hestrin, 1994; Poulson et al., 1997; Blake and Walter, 1999). The order of effectiveness of the dissolution enhancement of organic molecules on silicate minerals roughly matches the order of the metal-ligand stability constants (i.e. EDTA and citrate enhance dissolution kinetics more strongly than acetate) (Hausrath et al., 2009; Pokrovsky et al., 2009; Sillen, 1964), but is not in any simple way correlated to the formation of metal–ion complexes in solution. Clearly the dissolution enhancement is not the result of an equilibrium effect (i.e. increasing the solubility of the serpentine).

Identifying a catalyst for promoting the dissolution of metal-bearing silicate minerals under pH conditions that allow for the formation of solid carbonate phases would represent a significant breakthrough in the development of a direct aqueous carbonation process. With this work we have shown that dissolution-promoting organic anions such as citrate or oxalate can increase the dissolution rates of serpentine by three orders of magnitude over proton-promoted dissolution rates in the pH regime in which carbonate phases are stable. Extending the resources base of a mineral sequestration process to include serpentinized rocks greatly expands the geographical applicability of the technology as well as the overall CO_2 disposal potential of this technology (Krevor et al., 2009) and it is promising that these compounds specifically enhance the dissolution of serpentine, among the least reactive but most abundant of the ultramafic minerals.

We have not demonstrated that these salts can be used as catalytic solution additives. Further work is required to understand the conditions necessary to form carbonate phases in solutions containing these neutral organic salts. The formation of soluble metal–ligand complexes in the bulk solution will both reduce the metal activity in solution and reduce the proportion of "free" or uncomplexed ligand. Lowered magnesium activity will lead to a lower saturation index of the carbonate phases and more total metal cation will need to be in solutions to precipitate carbonate minerals. Reduced free ligand in solution will lower the dissolution enhancement effect (Liu et al., 2006; Grandstaff, 1986). As a result of these factors, the dissolution enhancement under process conditions will be lower than what has been observed in this study, if not entirely negated. It is clear, however, that the dissolution enhancement is not coupled in a linear fashion to the strength of the bulk solution metal–ion complex. Note that EDTA, which forms magnesium complexes several orders of magnitude more stable than oxalate and citrate, and could not be used as a catalyst, does not enhance the dissolution rate much more than these other anions (Fig. 4).

What has been identified are solution additives that greatly enhance the dissolution rate of serpentine in a pH regime in which carbonate phases are stable. This is the first test that must be passed by any potential catalyst in this process. Despite the potential limitations, the magnitude of the enhancement observed in this study is sufficiently large to encourage further investigation of the potential utility of such additives in a full carbonation process.

Acknowledgements

References

Allen, M., Smith, R., 1994. Dissolution of fibrous silicates in acid and buffered salt solutions. Minerals Engineering 7 (12), 1527–1537.

Bales, R.C., Morgan, J.J., 1985. Dissolution kinetics of chrysotile at ph 7 to 10. Geochimica et Cosmochimica Acta 49, 2281–2288.

Bennett, P.C., 1991. Quartz dissolution in organic-rich aqueous systems. Geochimica et Cosmochimica Acta 55, 1781–1797.

Bennett, P., Melcer, M., Siegel, D., Hassett, J., 1988. The dissolution of quartz in dilute aqueous solutions of organic acids at 25 °C. Geochimica et Cosmochimica Acta 52, 1521–1530.

Bethke, C.M., Yeakel, S., 2007. The Geochemist's Workbench Reference Manual, Release 7.0 Edition.

Blake, R., Walter, L., 1999. Kinetics of feldspar and quartz dissolution at 70–80 °C and near-neutral ph: effects of organic acids and NaCl. Geochimica et Cosmochimica Acta 63 (13/14), 2043–2059.

Bonifacio, E., Celi, L., Barberis, E., 2001. Effect of phosphate on the dissolution of serpentine. Soil Science 166 (10), 708–716.

Carey, J.W., Ziock Jr., H.-J.G.D.G., 2004. Reactivity of serpentine in CO_2-bearing solutions: application to CO_2 sequestration. Preparatory Paper American Chemical Society Division of Fuel Chemistry 49 (1), 371–372.

Chizmeshya, A., McKelvy, M., Wolf, G., Carpenter, R., Gormley, D., 2003. Enhancing the atomic-level understanding of CO_2 mineral sequestration mechanisms via advanced computational modeling. In: Tech. Rep. Arizona State University Center for Solid State Science. Arizona State University Center for Solid State Science.

Fein, J.B., Hestrin, J.E., 1994. Experimental studies of oxalate complexation at 80 °C: gibbsite, amorphous silica, and quartz solubilities in oxalate-bearing fluids. Geochimica et Cosmochimica Acta.

Gerdemann, S.J., O'Connor, W.K., Dahlin, D.C., Penner, L.R., Rush, H., 2007. Ex situ aqueous mineral carbonation. Environmental Science and Technology 41, 2587–2593.

Goff, F., Lackner, K., 1998. Carbon dioxide sequestering using ultramafic rocks. Environmental Geosciences 5 (3), 89–101.

Grandstaff, D., 1986. Rates of Chemical Weathering of Rocks and Minerals. Academic Press Inc (Chapter 3), pp. 439–452.

Gunnarsson, I., Arnorsson, S., 2000. Amorphous silica solubility and the thermodynamic properties of H_4SiO_4 in the range of 0 to 350 °C at Psat. Geochimica et Cosmochimica Acta 64 (13), 2295–2307.

Guthrie, G.D., Carey, J.W., Bergfeld, D., Chipera, S., Ziock, H.-J., Lackner, K., 2001. Geochemical aspects of the carbonation of magnesium silicates in aqueous medium. In: NETL Meeting on Carbon Capture and Sequestration.

Hänchen, M., Prigiobbe, V., Storti, G., Seward, T., Mazzotti, M., 2006. Dissolution kinetics of forsteritic olivine at 90 to 150 °C including effects of the presence of CO_2. Geochimica et Cosmochimica Acta 70 (17), 4403–4416.

Hänchen, M., Krevor, S., Lackner, K., Mazzotti, M., 2007. Validation of a population balance model for olivine dissolution. Chemical Engineering Science 62, 6412–6422.

Hänchen, M., Prigiobbe, V., Baciocchi, R., Mazzotti, M., 2008. Precipitation in the mg-carbonate system-effects of temperature and CO_2 pressure. Chemical Engineering Science 63, 1012–1028.

Hausrath, E., Neamann, A., Brantley, S., 2009. Elemental release rates from dissolving basalt and granite with and without organic ligands. American Journal of Science 309, 633–660.

House, K.Z., House, C.H., Schrag, D.P., Aziz, M.J., 2007. Electrochemical acceleration of chemical weathering as an energetically feasible approach to mitigating anthropogenic climate change. Environmental Science and Technology 41, 8454–8470.

Huijgen, W., Witkamp, G.-J., Comans, R., 2006. Mechanisms of aqueous wollastonite carbonation as a possible CO_2 sequestration process. Chemical Engineering Science 61, 4242–4251.

Huijgen, W.J., Comans, R.N., Witkamp, G.-J., 2007. Cost evaluation of CO_2 sequestration by aqueous mineral carbonation. Energy Conversion and Management 48, 1923–1935.

IPCC, 2005. Carbon Dioxide Capture and Storage. Cambridge University Press.

Jarvis, K., Carpenter, R., Windman, T., Kim, Y., Nunez, R., Alawneh, F., 2009. Reaction mechanisms for enhancing mineral sequestration of CO_2. Environmental Science and Technology 43 (16), 6314–6319.

Kakizawa, M., Yamasaki, A., Yanagisawa, Y., 2001. A new CO_2 disposal process via artificial weathering of calcium silicate accelerated by acetic acid. Energy 26, 341–354.

Kim, H., Lee, D., Fan, L., Park, A., 2009. Synthesis of iron-based chemical looping sorbents integrated with ph swing carbon mineral sequestration. Journal of Nanoscience and Nanotechnology 9 (12), 7422–7427.

Kline, W., Fogler, H., 1981. Dissolution kinetics: catalysis by salts. Journal of Colloid and Interface Science 82 (1), 103–115.

Krevor, S., Graves, C., Gosen, B.V., McCafferty, A., 2009. Mapping the mineral resource base for mineral carbon-dioxide sequestration in the conterminous United States. In: USGS Data Series 414. U.S. Geological Survey.

Lackner, K.S., Wendt, C.H., Butt, D.P., Joyce, E.L., Sharp, D.H., 1995. Carbon dioxide disposal in carbonate minerals. Energy 20 (11), 1152–1170.

Leblanc, S., Fogler, H., 1987. Population balance modeling of the dissolution of polydisperse solids: rate limiting regimes. AIChE Journal 33 (1), 54–63.

Liu, Y., Olsen, A.A., Rimstidt, J.D., 2006. Mechanism for the dissolution of olivine series minerals in acidic solutions. American Mineralogist 91, 455–458.

Maroto-Valer, M., Fauth, D., Kuchta, M., Zhang, Y., Andresen, J., 2005. Activation of magnesium rich minerals as carbonation feedstock materials for CO_2 sequestration. Fuel Processing Technology 86, 1627–1645.

Mavredaki, E., Stathoulopoulou, A., Neofotistou, E., Demadis, K.D., 2007. Environmentally benign chemical additives in the treatment and chemical cleaning of process water systems: implications for green chemical technology. Desalination 210, 257–265.

Morey, G., Foruier, R., Rowe, J., 1964. The solubility of amorphous silica at 25 °C. Journal of Geophysical Research 69 (10), 1995–2002.

Newall, P., Clarke, S., Haywood, H., Scholes, H., Clarke, N., King, P., Barley, R., 1999. CO_2 storage as carbonate minerals. In: Tech. Rep. International Energy Agency PH3/17, IEA.

Oelkers, E.H., Schott, J. (Eds.), 2009. Thermodynamics and Kinetics of Water-Rock Interaction, vol. 70 of Reviews in Mineralogy and Geochemistry. Mineralogical Society of America.

Olsen, A.A., Rimstidt, J.D., 2008. Oxalate-promoted forsterite dissolution at low ph. Geochimica et Cosmochimica Acta 72, 1758–1766.

Palandri, J.L., Kharaka, Y.K., 2004. A compilation of rate parameters of water-mineral interaction kinetics for application to geochemical modeling. In: USGS Open File Report 2004-1068. U.S. Geological Survey.

Park, A.-H.A., Fan, L.-S., 2004. CO_2 mineral sequestration: physically activated dissolution of serpentine and ph swing process. Chemical Engineering Science 59, 5241–5247.

Pokrovsky, O., Shirokova, L., Benezeth, P., Schott, J., Golubev, S., 2009. Effect of organic ligands and heterotrophic bacteria on wollastonite dissolution kinetics. American Journal of Science 309, 731–772.

Poulson, S.R., Drever, J.I., Stillings, L.L., 1997. Aqueous Si-oxalate complexing, oxalate adsorption onto quartz, and the effect of oxalate upon quartz dissolution rates. Chemical Geology 140, 1–7.

Seifritz, W., 1990. CO_2 disposal by means of silicates. Nature 345 (6275), 486.

Sillen, L.G., 1964. Stability Constants of Metal–Ion Complexes, Chemical Society, London. Special Publication no. 17. Royal Society of Chemistry.

Stoll, V., Blanchard, J., 1990. Buffers: Principles and Practice, Chapter 6 in Methods in Enzymology. Academic Press Inc.

Teir, S., Revitzer, H., Eloneva, S., Goelholm, C.-J., Zevenhoven, R., 2007. Dissolution of natural serpentinite in mineral and organic acids. International Journal of Mineral Processing 83, 36–46.

White, A., Brantley, S. (Eds.), 1995. Chemical Weathering Rates of Silicate Minerals, vol. 31 of Reviews in Mineralogy. Mineralogical Society of America.

Wogelius, R.A., Walther, J.V., 1991. Olivine dissolution at 25 °C: effects of ph, CO_2, and organic acids. Geochimica et Cosmochimica Acta 55, 943–954.